# Comparing adaptation strategies in MRI-guided online adaptive radiotherapy for prostate cancer: implications for treatment margins

Dassen, M.G.; Janssen, T.; Kusters, M.; Pos, F.; Kerkmeijer, L.G.W.; Heide, U.A. van der; Bijl, E. van der

Radiotherapy and Oncology 186 (2023) 109761

Contents lists available at ScienceDirect

Radiotherapy and Oncology

journal homepage: www.thegreenjournal.com

Original Article

# Comparing adaptation strategies in MRI-guided online adaptive radiotherapy for prostate cancer: Implications for treatment margins

Mathijs G. Dassen [a,1], Tomas Janssen [a], Martijn Kusters [b], Floris Pos [a], Linda G.W. Kerkmeijer [b], Uulke A. van der Heide [a], Erik van der Bijl [b,*]

[a] Department of Radiation Oncology, The Netherlands Cancer Institute, Amsterdam; and [b] Department of Radiation Oncology, Radboud University Medical Center, Nijmegen, the Netherlands

ARTICLE INFO

*Article history:*
Received 11 January 2023
Received in revised form 26 May 2023
Accepted 15 June 2023
Available online 20 June 2023

*Keywords:*
Prostate cancer
Margins
MRI-guided
Online adaptive radiotherapy
Intra-fraction motion

ABSTRACT

*Purpose:* To quantify the difference in accuracy of adapt-to-position (ATP), adapt-to-rotation (ATR) and adapt-to-shape (ATS) workflows used in MRI-guided online adaptive radiotherapy for prostate carcinoma (PCa) by evaluating the margins required to accommodate intra-fraction motion of the clinical target volumes for prostate (CTVpros), prostate including seminal vesicles (CTVpros + sv) and gross tumor volume (GTV).

*Materials and methods:* Clinical delineations of the CTVpros, CTVpros + sv and GTV of 24 patients with intermediate- and high-risk PCa, treated using ATS on a 1.5 T MR-Linac, were used for analysis. Delineations were available pre- and during beam-on. To simulate ATP and ATR workflows, we automatically generated the structures associated with these workflows using rigid transformations from the planning-MRI to the daily online MRIs. Clinical GTVs were analyzed as ATR GTVs and only ATP GTVs were simulated. Planning target volumes (PTVs) were generated with isotropic margins ranging 0.0–5.0 mm. The volumetric overlap was calculated between these PTVs and their corresponding clinical delineation on the MRI acquired during beam-on and averaged over all treatment fractions.

*Results:* The PTV margin required to cover > 95% of the CTVpros was equal (2.5 mm) for all workflows. For the CTVpros + sv, this margin increased to 5.0, 4.0 and 3.5 mm in the ATP, ATR and ATS workflow, respectively. GTV coverage improved from ATP to ATR for margins up to 4.0 mm.

*Conclusion:* ATP, ATR and ATS workflows ensure equal coverage of the CTVpros for the current clinical margins. For the CTVpros + sv, ATS showed optimal performance. GTV coverage improves by additional adaptations to prostate rotations.



In online adaptive radiotherapy for treatment of prostate carcinoma (PCa) either cone-beam computed tomography (CBCT) or magnetic resonance imaging (MRI) can be used for daily plan adaptation to account for inter-fractional variations in anatomy over the course of treatment [1–4]. The most important benefits offered by MRI-guided systems are its superior soft tissue contrast and the possibility to obtain images during treatment delivery. As a result, MRI-guided radiotherapy minimizes errors in inter-fraction set-up and potentially allows for intra-fraction motion correction using continuous MRI acquisition, thereby reducing planning target volume (PTV) margins used to ensure target dose delivery [5–10].

In MRI-guided online adaptive radiotherapy for PCa different workflows are available and used for online plan adaptation. The options range from a workflow where the daily plan is adapted by a rigid shift based on the online patient position, known as the adapt-to-position (ATP) workflow, to a workflow in which the daily plan is fully re-optimized with manually updated delineations on daily imaging, known as the adapt-to-shape (ATS) workflow [11]. The time-interval between daily imaging and treatment delivery in the ATS workflow is prolonged, which may negatively affect the accuracy of the improved delineation during irradiation due to any occurred intra-fraction motion [12–15]. As an intermediate between the ATP and ATS workflow the adapt-to-rotation (ATR) workflow was introduced, to balance speed and accuracy, which corrects for translations and rotations of the targets.

Next to intra-fraction motion, the accuracy of the delineations in each workflow during irradiation is also affected by prostate and seminal vesicles inter-fraction motion. While the prostate volume is known to increase in volume along the course of treatment,

* Corresponding author at: Department of Radiation Oncology, Radboud University Medical Center, Nijmegen, The Netherlands Geert Grooteplein Zuid 10, 6525 GA, Nijmegen, the Netherlands.

*E-mail addresses:* t.dassen@nki.nl (M.G. Dassen), erik.vanderbijl@radboudumc.nl (E. van der Bij.

[1] Department of Radiation Oncology, The Netherlands Cancer Institute, Amsterdam, The Netherlands Plesmanlaan 121, 1066 CX, Amsterdam.

https://doi.org/10.1016/j.radonc.2023.109761
0167-8140/

the seminal vesicles may show considerable rotations and deformations between fractions [16,17]. For this reason, the PTV margins required to cover for both these inter- and intra-fractional geometrical uncertainties may be different among the different workflows and depend on the specific motion patterns of the defined target volume. The potential benefit of full online re-contouring, as performed in the ATS workflow, is that it should allow for smaller PTV margins compared to ATP or ATR workflows and as such warrants this more time-consuming workflow. Since the PTV generally overlaps with rectum and bladder volumes, ATS should also reduce dose to these healthy tissue structures. In addition, it has recently been demonstrated that focal boosting treatment regimens improve outcome in patients treated for localized PCa [18]. Focal dose-escalation may also increase the need for a highly accurate adaptation strategy to ensure GTV coverage of the boosted dose area. However, the benefit of the ATS workflow compared to the ATP or ATR workflow in terms of PTV margins in MRI-guided online adaptive radiotherapy for PCa still needs to be established.

The aim of this study was to quantify the difference in accuracy of online adaptive workflows used in MRI-guided adaptive radiotherapy for PCa by evaluating the margins required to accommodate intra-fraction motion of the GTV, prostate and prostate including seminal vesicles in ATP, ATR and ATS workflows. In addition, PTV-overlap with rectum and bladder volumes was analyzed in order to evaluate the impact of each of these workflows on the OARs.

## Materials and methods

### *Patient data*

In this study the clinical delineations of 26 patients with intermediate- and high-risk PCa were included. No patients with seminal vesicle invasion were included. The patients were treated between March 2021 and December 2021 at the Radboud University Medical Center (Radboud UMC, Nijmegen, The Netherlands) on a 1.5 T Unity MR-Linac (Elekta AB, Stockholm, Sweden) in 5 fractions within the hypoFLAME 2.0 trial (NCT04045717) [19]. All patients provided written informed consent.

### *Analyzed online adaptive workflows: ATP, ATR, ATS*

In MRI-guided online adaptive radiotherapy for PCa various workflows for daily plan adaptation are in clinical use with small variations in clinical practice. Here we define the workflows mentioned in the introduction such as we analyzed them in the current work. In the ATP workflow, the daily MRI is used to update the isocenter position of the reference plan to the daily patient position (a.k.a. a virtual couch shift) using a translations-only registration, followed by a re-optimization of the plan. In the ATR workflow, the target contours are adjusted using rigid translations and rotations to align with the daily MRI after which the daily plan is re-optimized. In both these workflows, delineations are rigidly propagated from reference to daily images. In the ATS workflow all contours are inspected and where necessary corrected slice by slice after being propagated to the daily MRI.

### *Clinical ATS workflow*

Patients underwent a computed tomography (CT) for dose calculation only and a 3 T simulation MRI (planning-MRI, 3D T2w, 1.0x1.0x2.0 $mm^3$) prior to the first fraction of radiation delivery for delineation of target volumes and organs at risk (OARs). All targets were delineated on the planning-MRI by a radiation oncologist in Mirada (version 1.4.0, Mirada Medical Ltd, Oxford, United Kingdom). Multi-parametric MRI including ADC was available for all patients. Gross tumor volume (GTV) was defined as the visible tumor nodule(s) on multi-parametric MRI. The clinical target volume ($CTV_{pros}$) included the whole prostate gland and GTV + 4 mm margin to cover for any microscopic extensions, excluding OARs. Seminal vesicles were contoured up to 2 cm proximal to the $CTV_{pros}$ and were defined as a second CTV ($CTV_{sv}$).

At each fraction of treatment, a daily 3D T2w MRI (adaptation-MRI) was acquired, with a field-of-view (FOV) of 400x400x300 $mm^3$ and a voxel spacing of 0.83x0.83x1.0 $mm^3$. All contours of the planning-MRI were rigidly propagated to the adaptation-MRI by Monaco (version 5.40.1, Elekta AB, Stockholm, Sweden) and subsequently together manually shifted and rotated to get the best alignment with the daily scan. The CTVs were then manually adjusted by a radiation oncologist and the GTV was only adjusted if visible on the adaptation-MRI or in case the GTV extended outside the CTV after re-delineation. In addition, OARs were adjusted within the first 2 cm around the clinical CTV-PTV margin (5.0 mm), after which full plan re-optimization was performed in Monaco.

Before beam-on, another T2w MRI was acquired (position-verification-MRI) to check for any intra-fraction motion during re-delineation. This scan was compared to the adaptation-MRI and in case of an observed shift of $\geq$ 2.0 mm of the CTV a shift was applied to the daily re-optimized plan [20]. Thereafter, treatment delivery was started. At approximately half of the beam-on time, an additional MRI was acquired (during-MRI). In between fractions the treatment progress was evaluated by adapting the contours from the adaptation-MRI to the during-MRI using an ATS procedure performed by an RTT with visual inspection of a radiation oncologist, which were used for recalculation of the dose on the during-MRI. The delineations of rectum and bladder on the during-MRI were included in this analysis. The adaptation-, position-verification- and during-MRI were all acquired using the same MRI sequence. Fig. 1 provides an overview of the time required for all steps undertaken in the clinical workflow. These timings were also used to estimate the time required for performing the ATP and ATR workflow.

### *Analyzed target contours*

For the purpose of this study, all delineations of the $CTV_{pros}$, the CTV including both $CTV_{pros}$ and $CTV_{sv}$ ($CTV_{pros+sv}$) and GTV were extracted from the clinically available data. Since clinically ATS was used (potentially with a shift based on the position-verification-MRI), we will denote these as $CTV^{ATS}_{pros}$ and likewise for the other structures. Since the ATP and ATR workflows were not clinically performed, we automatically generated the CTV structures associated with these workflows. To create the $CTV^{ATP}_{pros}$, we performed a translations-only registration of the mask of the clinical planning delineation ($CTV^{Plan}_{pros}$) to the re-delineated $CTV^{ATS}_{pros}$ on the daily adaptation-MRI (Fig. 2). For the $CTV^{ATR}_{pros}$, rigid registrations using translations and rotations were performed, likewise. Similarly, the $CTV^{ATP}_{pros+sv}$ and $CTV^{ATR}_{pros+sv}$ structures were created. As a result, $CTV_{pros}$ and $CTV_{pros+sv}$ structures were available for all investigated adaptation strategies. All registrations (binary maps, correlation ratio) were performed automatically using an in-house developed software package (Match42) and were visually checked for clinical acceptability.

For the GTV, we only considered two workflows for analysis. In the clinical workflow the $GTV^{Plan}$ was propagated alongside with the $CTV^{Plan}_{pros}$ to the daily adaptation-MRI using rigid translations and manual rotations (similar to the ATR workflow). Subsequently, the $GTV^{Plan}$ was only adjusted if visible. Since this is generally chal-

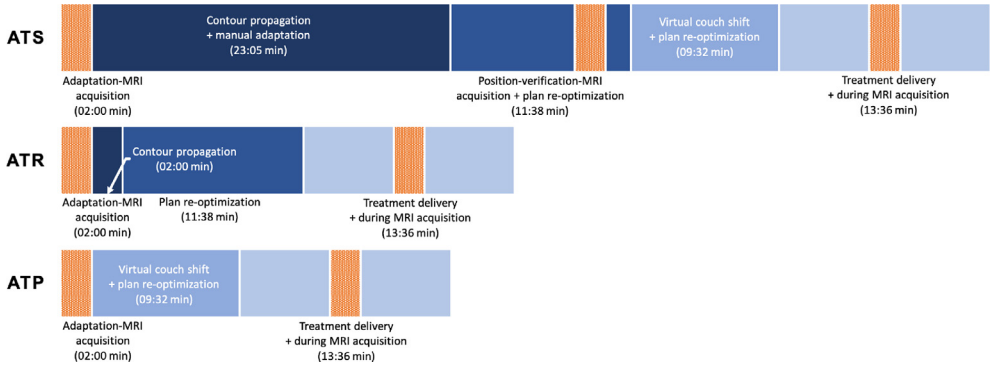


**Fig. 1.** A timeline showing the mean time required for each step in the clinical ATS workflow (top) starting with the acquisition of the adaptation-MRI (dotted), followed by the steps listed from left to right. The position-verification-MRI (dotted) was acquired towards the end of plan re-optimization and the during-MRI (dotted) was acquired approximately half-way during treatment delivery, both with an acquisition time of 02:00 min. The mean total treatment time was 54.5 min (sd 8.8 min; range 36.8 – 94.6 min).The timeline of the ATP (bottom) and ATR (middle) workflow were estimated based on the time required for each step in the clinical workflow. The estimated total treatment time was 25.1 min and 29.2 min for the ATP and ATR workflow, respectively.

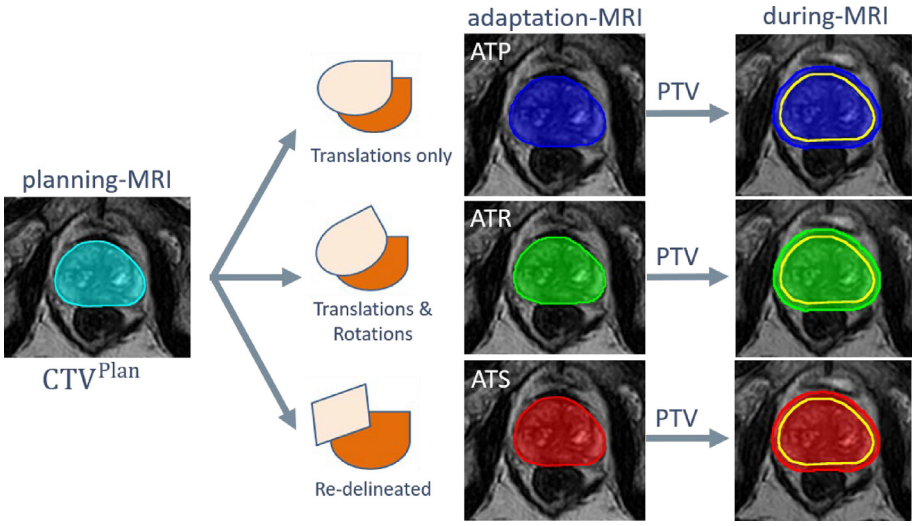


**Fig. 2.** Schematic overview of the delineated and simulated CTV contours. The CTV of the planning-MRI ($CTV^{Plan}$) and the re-delineated CTVs of the adaptation- and during-MRI were extracted from the clinical data. The $CTV^{ATP}$ and $CTV^{ATR}$ were generated by either a rigid translations-only registration (ATP) or using both translations and rotations (ATR). PTVs were created for each CTV for the range of margins up to 5.0 mm. Subsequently, the volumetric overlap of the PTV with its corresponding delineation on the during-MRI (indicated by the yellow contour within the PTVs) was evaluated for each strategy.

lenging on T2w MRIs, the $GTV^{Plan}$ was not adjusted in the majority of patients (in one fraction of one patient the GTV extended outside the prostate after re-delineation of the $CTV_{pros}$, and was therefore edited; in one other patient the GTV was edited on the first fraction, after which this edit was rigidly propagated to the remaining fractions). Therefore, we evaluated these clinical GTV delineations as $GTV^{ATR}$ structures and only created additional $GTV^{ATP}$ structures. For this purpose, we applied the translation of the $CTV^{Plan}_{pros}$ to the $GTV^{Plan}$ on the daily adaptation-MRI.

*Analysis*

The clinical and simulated CTV and GTV contours were used to generate PTVs with isotropic margins ranging from 0.0 to 5.0 mm in steps of 0.5 mm using a rolling-ball algorithm in Match42 [21]. We will use the following notation: $CTV^{ATS}_{pros} \xrightarrow{3mm} PTV^{ATS,3mm}_{pros}$, to denote a 3.0 mm expansion of the $CTV_{pros}$. Subsequently, these PTVs were compared to their corresponding clinical delineation on the during-MRI (e.g. $CTV^{During}_{pros}$). Continuing our example, the volumetric overlap between the PTV and its corresponding contour on the during-MRI is then given by:

$$Overlap^{ATS,\ 3mm}_{pros}(\%) = \frac{Vol\,(PTV^{ATS,\ 3mm}_{pros} \cap CTV^{During}_{pros})}{Vol\,(CTV^{During}_{pros})} \cdot 100\%$$

Coverage was calculated over the complete course of treatment by calculating the mean volumetric overlap per patient over 5 fractions. This calculation was performed for each target structure for each PTV margin. For the $CTV_{pros}$ and $CTV_{pros+sv}$, we determined the PTV margin that showed > 95% coverage of the $CTV^{During}_{pros}$ in 90% of the patients. In case of the GTV, this criterion was reduced to > 90% coverage of the $GTV^{During}$ in 90% of the patients, because of a smaller total volume of the GTV compared to the CTV [22]. Moreover, in focal boosting, the dose to the GTV is escalated on top of the dose to the CTV which results in a more gradual dose gradient outside

the GTV and as such warrants this relaxed criterion. Robustness of these criteria was assessed by analyzing the change in coverage in case of analyzing 85% and 95% instead of 90% of the patients.

In addition to our analysis of PTV coverage of the CTVs and GTV, we did also analyze the impact of each adaptation strategy on PTV-overlap with the OARs. In this case, the volumetric overlap of the $PTV_{pros}$ and $PTV_{pros+sv}$ as defined for each workflow and margin were evaluated with respect to the rectum and bladder delineations on the during-MRI. Similar to the analysis of target coverage, we calculated the mean volumetric overlap per patient over 5 fractions. Data analysis was performed in a commercial statistical software package (SPSS, version 27, SPSS Inc.).

## Results

Twenty-six patients were included for analysis. In two patients, data was missing and these were therefore excluded. In these 24 patients, a total of 120 fractions were analyzed. The mean time-interval between the adaptation-MRI and the during-MRI was 46.7 min (sd 8.7 min; range 27.9 – 85.4 min).

Fig. 3A and 3B show boxplots of the coverage of the $CTV^{During}_{pros}$ and $CTV^{During}_{pros+sv}$ as defined for each adaptation strategy for PTV margins between 0.0 and 5.0 mm. The margin for the $PTV_{pros}$ that was required to cover > 95% of the $CTV^{During}_{pros}$ in 90% of the patients (excluding 3 patients) was equal in each adaptive workflow. Based on this criterion a PTV margin of 2.5 mm would be sufficient in each workflow to cover for any intra-fraction motion of the prostate during treatment delivery. In case the seminal vesicles are included in the CTV ($CTV_{pros+sv}$), the PTV margin that was required to ensure > 95% coverage of the $CTV^{During}_{pros+sv}$ in 90% of the patients increased to 5.0 mm for the $PTV^{ATP}_{pros+sv}$, whereas the PTV margin for that same criterion was only 4.0 mm for the $PTV^{ATR}_{pros+sv}$ and 3.5 mm for the $PTV^{ATS}_{pros+sv}$. In addition, Fig. 3C shows the boxplot of the coverage of the $GTV^{During}$ for the $GTV^{ATP}$ and $GTV^{ATR}$ for the same range of margins up to 5.0 mm. In this case, a 4.0 mm margin was required to reach the coverage criterion of 90% in both the ATP and ATR workflow. Results on the robustness of these criteria are provided in Figure S1 (excluding 2 patients) and Figure S2 (excluding 4 patients) in the supplementary material.

Fig. 4 shows boxplots of the volumetric overlap of the $PTV_{pros}$ with rectum (Fig. 4A) and bladder (Fig. 4C) and similarly for the $PTV_{pros+sv}$ (Fig. 4B and 4D) as defined for each adaptive workflow for the range of PTV margins between 0.0 and 5.0 mm. No difference in volumetric overlap was observed between the workflows for both the $PTV_{pros}$ and $PTV_{pros+sv}$ for any PTV margin.

## Discussion

The aim of this study was to quantify the relative benefit of different online adaptive workflows in MRI-guided online adaptive radiotherapy for PCa. Our results show that in case the CTV only encompasses the prostate volume, both the ATR and ATS workflow did not reduce the required PTV margin compared to the ATP workflow. Especially for the typical margins used in current clinical practice, which are between 3.0 and 5.0 mm, the difference in target coverage between the workflows is negligible [19,23,24]. In case the CTV also includes, (a part of) the seminal vesicles, however, the ATS workflow would allow for a margin reduction of 0.5 mm and 1.5 mm compared to the ATR and ATP workflow, respectively.

For the GTV, the ATR workflow did improve GTV coverage compared to the ATP workflow in case of margins up to 4.0 mm. However, the margin that could ensure GTV coverage of > 90% in 90% of

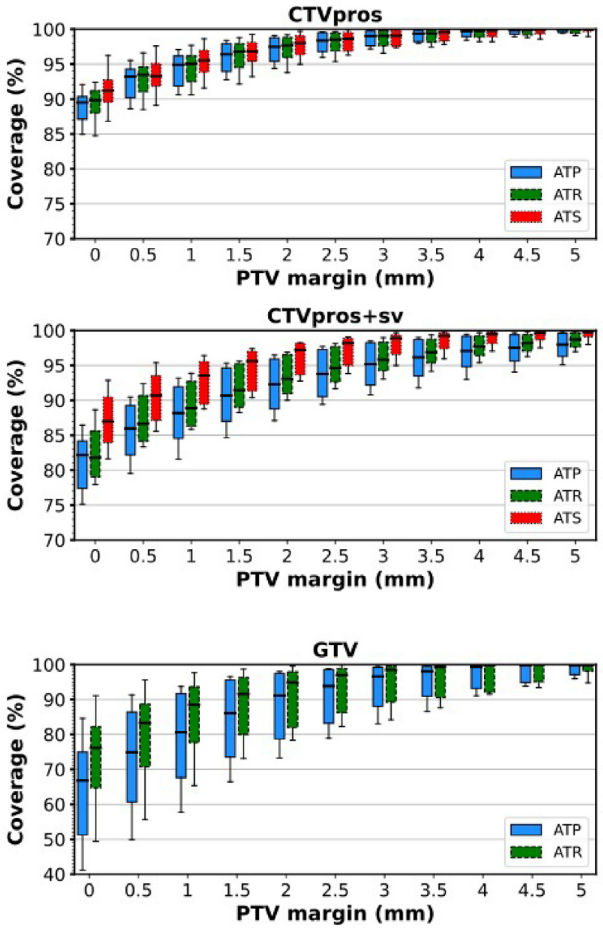


**Fig. 3.** Boxplots of the coverage of the A) $CTV_{pros}$, B) $CTV_{pros+sv}$ and C) GTV for margins up to 5.0 mm for ATP, ATR and ATS workflows. Boxes indicate the interquartile range (IQR), median values are indicated in black. The whiskers indicate the 10th-percentile and 90th-percentile interval. Coverage was defined as the percentage of the CTV/GTV as defined on the during-MRI that was covered by its corresponding PTV as defined on the adaptation- MRI.

the population was 4.0 mm in both the ATP and ATR workflow. In the FLAME trial, however, no margins were applied to the GTV to ensure GTV planned boost dose delivery. Moreover, Van Schie et al. showed that due to a strict adherence to dose constraints to the OARs the median planned D98% to the GTV in the FLAME trial was 84.7 Gy instead of the aimed prescribed dose of 95 Gy and similar results were presented for the hypo-FLAME trial [19,25]. Consequently, when adding a margin to the GTV, the maximum feasible D98% for the GTV plus margin would likely be lower compared to the GTV without margin in order to satisfy organ at risk constraints.

PTV-overlap of both the $PTV_{pros}$ and $PTV_{pros+sv}$ with rectum and bladder volumes did not show any differences between ATP, ATR and ATS workflows. Both inter- and intra-fraction geometric variations of the prostate and seminal vesicles are correlated with variations in bladder and rectal filling [26,27]. As a result, the choice for any adaptation strategy does not influence the dose to adjacent OARs other than via the necessary treatment margins in case of a homogeneous CTV dose. In case of dose differentiation within the CTV (e.g. focal boosting), however, this analysis would require evaluation of accumulated dose.

In addition to accounting for target motion, the PTV margin should also consider other uncertainties such as uncertainties in gantry positioning, image alignment and delineation uncertainty, which were not incorporated in the margins presented in this

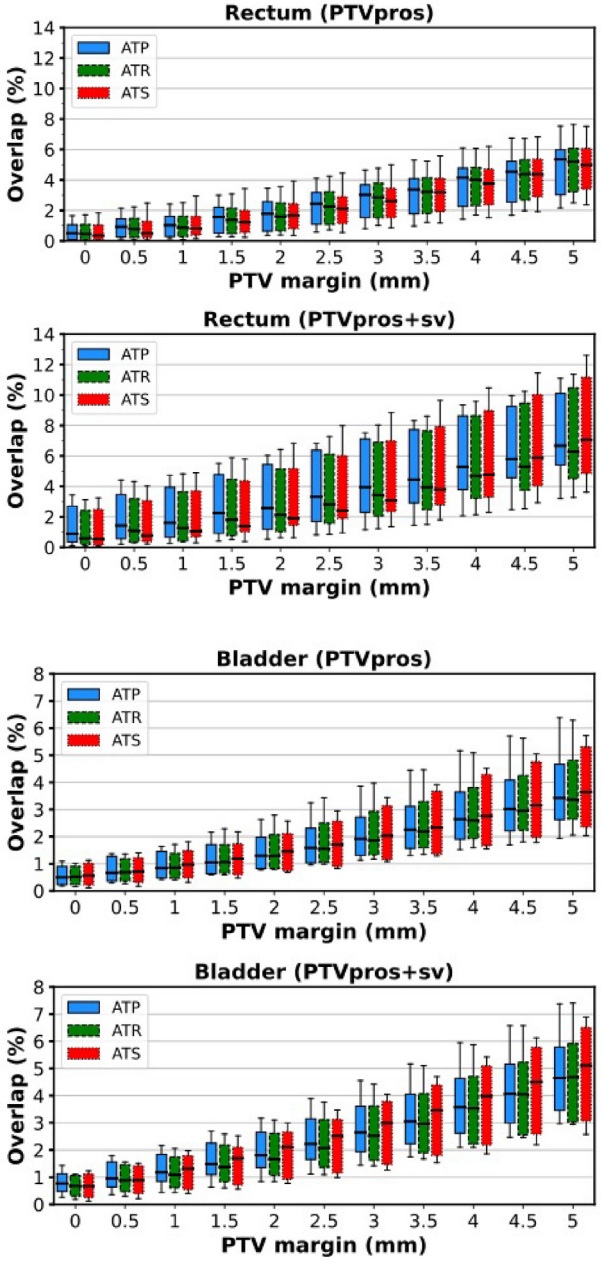


**Fig. 4.** Boxplots of the volumetric overlap of the A) $PTV_{pros}$ with rectum, B) $PTV_{pros+sv}$ with rectum, C) $PTV_{pros}$ with bladder and D) $PTV_{pros+sv}$ with bladder for PTV margins up to 5.0 mm for ATP, ATR and ATS workflows. Boxes indicate the IQR, median values are indicated in black. The whiskers indicate the 10th-percentile and 90th-percentile interval. Volumetric overlap was defined as the percentage of the OAR as defined on the during-MRI that overlapped with each PTV as defined on the adaptation-MRI.

study. It could be argued that in the ATS workflow the delineation uncertainty acquires a random component due to re-delineation, which is not present in the ATP and ATR workflow. The other factors would similarly affect the clinical PTV margin in each workflow. We therefore argue that our results do reflect the actual differences in the PTV margins needed in each of the evaluated workflows.

Our study did have other limitations. Firstly, the ATP and ATR workflow were simulated by rigid registrations of the planning contours to the re-delineated ATS contours on the daily adaptation-MRI used for the irradiated plan. As a consequence of this methodology, the time-interval between plan adaptation and treatment delivery in the simulated ATP and ATR workflows was equal to the clinical ATS workflow. Whereas this time-interval may be larger than clinical practice, it is unclear whether this may have led to an over- or underestimation of target coverage in both these simulated workflows. A study by Ballhausen et al. demonstrated that during fractions the prostate tends to show a drift with increasing variance over time, therefore suggesting to opt for a shorter total time per fraction in order to reduce the impact of intra-fraction motion [28]. Secondly, the during-MRI, acquired at approximately half of the beam-on time, was used as a surrogate for any intra-fraction displacements of the CTV during treatment delivery [29]. Alternatively, cine-MRI imaging acquired during the total beam-on phase could potentially improve evaluation of target coverage [30]. Lastly, in clinical practice the PTV margin may occasionally be reduced posteriorly towards 3.0 mm in order to reduce dose towards rectum [31]. In addition, a different PTV margin may be applied to the prostate compared to the seminal vesicles. However, in our clinical practice we only use isotropic margins and therefore we did only analyze margins as such and we did not analyze the seminal vesicles as a separate CTV.

This study showed that for the CTV including only prostate equal PTV margins can be applied in ATP, ATR and ATS workflows. Using the ATP or ATR workflow instead of ATS would remove the need for online re-delineation and will therefore reduce the total time per fraction by approximately 20 minutes based on our data. De Muinck Keizer et al. also reported on the time required for online re-delineation, which was performed in approximately 10 minutes in their clinical practice [12]. Because of a shorter time-interval between daily imaging and irradiation in these workflows, correction for any intra-fraction shift may also no longer be necessary which would allow for an additional reduction of approximately 10 minutes. Consequently, this would result in less burden to the patient and allow for an improved utilization of the treatment machine.

In addition, our study showed that for the CTV including prostate and seminal vesicles the ATS workflow allows for a margin reduction of 0.5 mm – 1.5 mm. Although in general smaller margins lead to a lower toxicity burden, as demonstrated for example by Kishan et al. for a 2 mm reduction leading to a decrease both GI and GU toxicity rates [10], evidence is currently lacking to determine the clinical benefit of reducing the PTV margin by 0.5 mm. One approach is to accept the additional time and resources of the ATS workflow aiming to minimize the risk of toxicity. Alternatively, one could also argue that a reduction of 0.5 mm does not outweigh these efforts. At this point, it becomes a cost-effectiveness issue in which institutes can define their preferences based on their resources and availability.

Methods for intra-fraction motion management on MRI-guided systems, such as gating and real-time tracking, would potentially allow for a further reduction of the PTV margins. Currently, MRI-guided beam-gated radiotherapy is available on the MRIdian MR-linac (ViewRay Inc, Cleveland, USA), whereas MRI-guided tracking methods still face some technical hurdles before clinical introduction [30,32]. Alternatively, Willigenburg et al. recently presented an adaptive workflow in which the fractional dose is divided into sub-fractions, thereby allowing for a reduction of the PTV margin to 2.0 mm (LR and CC) and 3.0 mm (AP) in case of dividing into two sub-fractions [33,34]. Our study showed that in case of an increased reduction of the PTV margin, re-contouring on daily imaging also becomes increasingly important to ensure target coverage during treatment.

In conclusion, this study showed that ATP, ATR and ATS workflows, used in MRI-guided online adaptive radiotherapy for PCa, can ensure equal coverage of the CTV including prostate only for the margins currently used in clinical practice. In case (a part of) the seminal vesicles are also included in the CTV the ATS workflow

showed optimal performance. GTV coverage improves by additional adaptation of the GTV to any prostate rotations for margins up to 4.0 mm, which could be of relevance for focal dose-escalation.

## Funding

This research has been funded by the KWF Dutch Cancer Society (project number 14338). The funding source was not involved in the design of the study, the collection, analysis and interpretation of the data, nor in the writing and decision to submit the article for publication.

## Conflict of interest

UAH: The department of radiation oncology of the Netherlands Cancer Institute receives research funding from Elekta AB and Philips Healthcare.

## Declaration of Competing Interest

The authors declare that they have no known competing financial interests or personal relationships that could have appeared to influence the work reported in this paper.

## Appendix A. Supplementary material

Supplementary data to this article can be found online at https://doi.org/10.1016/j.radonc.2023.109761.

## References

[1] Bertelsen AS, Schytte T, Møller PK, et al. First clinical experiences with a high field 1.5 T MR Linac. Acta Oncol 2019;58:1352–7. https://doi.org/10.1080/0284186X.2019.1627417.
[2] Tetar SU, Bruynzeel AM, Lagerwaard FJ, et al. Clinical implementation of magnetic resonance imaging guided adaptive radiotherapy for localized prostate cancer. Phys Imaging Radiat Oncol 2019;9:69–76. https://doi.org/10.1016/j.phro.2019.02.002.
[3] Byrne M, Archibal-Heeren B, Hu Y, et al. Varian ethos online adaptive radiotherapy for prostate cancer: early results of contouring accuracy, treatment plan quality, and treatment time. J Appl Clin Med Phys 2022;23:e13479.
[4] Zwart LG, Ong F, Ten Asbroek LA, et al. Cone-beam computed tomography-guided online adaptive radiotherapy is feasible for prostate cancer patients. Phys Imaging Radiat Oncol 2022;22:98–103. https://doi.org/10.1016/j.phro.2022.04.009.
[5] Rasch C, Barillot I, Remeijer P, et al. Definition of the prostate in CT and MRI: a multi-observer study. Int J Oncol Biol Phys 1999;43:57–66. https://doi.org/10.1016/S0360-3016(98)00351-4.
[6] Pathmanathan AU, Schmidt MA, Brand DH, et al. Improving fiducial and prostate capsule visualization for radiotherapy planning using MRI. J Appl Clin Med Phys 2018;20:27–36. https://doi.org/10.1002/acm2.12529.
[7] Pathmanathan AU, McNair HA, Schmidt MA, et al. Comparison of prostate delineation on multimodality imaging for MR-guided radiotherapy. BJR 2019;92:20180948. https://doi.org/10.1259/bjr.20180948.
[8] Nyholm T, Nyberg M, Karlsson MG, Karlsson M. Systematisation of spatial uncertainties for comparison between a MR and CT-based radiotherapy workflow for prostate treatments. Radiat Oncol 2009;4. https://doi.org/10.1186/1748-717X-4-54.
[9] Klüter S. Technical design and concept of a 0.35 T MR-Linac. Clin Transl Radiat Oncol 2019;18:98–101. https://doi.org/10.1016/j.ctro.2019.04.007.
[10] Kishan AU, Ma TM, Lamb JM, et al. Magnetic resonance imaging-guided vs computed tomography-guided stereotactic body radiotherapy for prostate cancer: The MIRAGE randomized clinical trial. JAMA Oncol 2023;9:365–73. https://doi.org/10.1001/jamaoncol.2022.6558.
[11] Winkel D, Bol GH, Kroon PS, et al. Adaptive Radiotherapy: the Elekta Unity MR-linac concept. Clin Transl Radiat Oncol 2019;18:54–9. https://doi.org/10.1016/j.ctro.2019.04.001.
[12] De Muinck Keizer DM, Kerkmeijer LG, Willigenburg T, et al. Prostate intrafraction motion during the preparation and delivery of MR-guided radiotherapy sessions on a 1.5T MR Linac. Radiother Oncol 2020;151:88–94. https://doi.org/10.1016/j.radonc.2020.06.044.
[13] De Muinck Keizer DM, Willigenburg T, Van Der Voort van Zyp JR, et al. Seminal vesicle intrafraction motion during the delivery of radiotherapy sessions on a 1.5 T MR-Linac. Radiother Oncol 2021;162:162–9. https://doi.org/10.1016/j.radonc.2021.07.014.
[14] Ruggieri R, Rigo M, Naccarato S, et al. Adaptive SBRT by 1.5 T MR-Linac for prostate cancer: on the accuracy of dose delivery in view of the prolonged session time. Phys Med 2020;80:34–41. https://doi.org/10.1016/j.ejmp.2020.09.026.
[15] Schaule J, Chamberlain M, Wilke L, et al. Intrafractional stability of MR-guided online adaptive SBRT for prostate cancer. Radiat Oncol 2021;16:189. https://doi.org/10.1186/s13014-021-01916-0.
[16] Ma TM, Neylon J, Casado M, et al. Dosimetric impact of interfraction prostate and seminal vesicle volume changes and rotation: A post-hoc analysis of a phase III randomized trial of MRI-guided versus CT-guided stereotactic body radiotherapy. Radiother Oncol 2022;167:203–10. https://doi.org/10.1016/j.radonc.2021.12.037.
[17] Alexander SE, McNair HA, Oelfke U, et al. Prostate volume changes during extreme and moderately hypofractionated magnetic resonance image-guided radiotherapy. *Clinical Oncology*, 2022. 22;S0936-6555(22)00177-7. https://doi.org/10.1016/j.clon.2022.03.022.
[18] Kerkmeijer LG, Groen VH, Pos FJ, et al. Focal boost to the intraprostatic tumor in external beam radiotherapy for patients with localized prostate cancer: Results of the FLAME randomized phase III trial. J Clin Oncol 2021;39:787–96. https://doi.org/10.1200/JCO.20.02873.
[19] Draulans C, Van Der Heide UA, Haustermans K, et al. Primary endpoint analysis of the multicentre phase II hypo-FLAME trial for intermediate and high risk prostate cancer. Radiother Oncol 2020;147:92–8. https://doi.org/10.1016/j.radonc.2020.03.015.
[20] De Muinck Keizer DM, Der Voort V, van Zyp JR, Breugel D-V, et al. On-line daily plan optimization combined with a virtual couch shift procedure to address intrafraction motion in prostate magnetic resonance guided radiotherapy. Phys Imaging Radiat Oncol 2021;19:90–5. https://doi.org/10.1016/j.phro.2021.07.010.
[21] Stroom JC, Storchi PR. Automatic calculation of three-dimensional margins around treatment volumes in radiotherapy planning. Phys Med Biol 1997;42. https://doi.org/10.1088/0031-9155/42/4/011.
[22] Kensen CM, Janssen TM, Betgen A, et al. Effect of intrafraction adaptation on PTV margins for MRI guided online adaptive radiotherapy for rectal cancer. Radiat Oncol 2022;17:110. https://doi.org/10.1186/s13014-022-02079-2.
[23] Brand DH, Tree AC, Ostler P, et al. Intensity-modulated fractionated radiotherapy versus stereotactic body radiotherapy for prostate cancer (PACE-B): acute toxicity findings from an international, randomised, open-label, phase 3, non-inferiority trial. Lancet Oncol 2019;20:1531–43. https://doi.org/10.1016/S1470-2045(19)30569-8.
[24] Ma TM, Jm L, Casado M, et al. Magnetic resonance imaging-guided stereotactic body radiotherapy for prostate cancer (mirage): a phase iii randomized tiral. BMC Cancer 2021;21. https://doi.org/10.1186/s12885-021-08281-x.
[25] Van Schie MA, Janssen TM, Eekhout D, et al. Knowlegde-based assessment of focal dose escalation treatment plans in prostate cancer. Int J Radiat Oncol Biol Phys 2020;108:1055–62. https://doi.org/10.1016/j.ijrobp.2020.06.072.
[26] Frank SJ, Dong L, Kudchadker RJ, et al. Quantification of prostate and seminal vesicle interfraction variation during IMRT. Int J Radiat Oncol Biol Phys 2008;71:813–20. https://doi.org/10.1016/j.ijrobp.2007.10.028.
[27] Mak D, Gill S, Paul R, et al. Seminal vesicle interfraction displacement and margins in image guided radiotherapy for prostate cancer. Radiat Oncol 2012;7:139. https://doi.org/10.1186/1748-717X-7-139.
[28] Ballhausen H, Li M, Hegemann N, et al. Intra-fraction motion of the prostate is a random walk. Phys Med Biol 2015;60:549–63. https://doi.org/10.1088/0031-9155/60/2/549.
[29] Janssen TM, Van Der Heide UA, Remeijer P, et al. A margin recipe for the management of intra-fraction target motion in radiotherapy. Phys Imaging Radiat Oncol 2022;24:159–66. https://doi.org/10.1016/j.phro.2022.11.008.
[30] De Muinck Keizer DM, Kerkmeijer LG, Maspero M, et al. Soft-tissue prostate intrafraction motion tracking in 3D cine-MR for MR-guided radiotherapy. Phys Med Biol 2019;64. https://doi.org/10.1088/1361-6560/ab5539.
[31] Tree AC, Ostler P, Van der Voet H, et al. Intensity-modulated radiotherapy versus stereotactic body radiotherapy for prostate cancer (PACE-B): 2-year toxicity results from an open-label, randomised, phase 3 non-inferiority trial. Lancet Oncol 2022;23:1308–20. https://doi.org/10.1016/S1470-2045(22)00517-4.
[32] Wahlstedt I, Andratschke N, Behrens CP, et al. Gating has a neglible impact on dose deliverd in MRI-guided online adaptive radiotherapy of prostate cancer. Radiother Oncol 2022;170:205–12. https://doi.org/10.1016/j.radonc.2022.03.013.
[33] Lagerwaard F, Bohoudi O, Tetar S, et al. Combined inter- and intrafractional plan adaptation using fraction partitioning in magnetic resonance-guided radiotherapy delivery. Cureus 2018;10:e2434.
[34] Willigenburg T, Zachiu C, Bol GH, et al. Clinical application of a sub-fractionation workflow for intrafraction re-planning during prostate radiotherapy treatment on a 1.5 Tesla MR-Linac: A practical method to mitigate intrafraction motion. Radiother Oncol 2022;176:25–30. https://doi.org/10.1016/j.radonc.2022.09.004.